Available online at www.sciencedirect.com

SciVerse ScienceDirect

Journal of the European Ceramic Society 32 (2012) 657–663

www.elsevier.com/locate/jeurceramsoc

Formation of TiO_2 nano fibers on a micro-channeled Al_2O_3–ZrO_2/TiO_2 porous composite membrane for photocatalytic filtration

Hyun-Jin Hong, Swapan Kumar Sarkar, Byong-Taek Lee *

Department of Biomedical & Materials, School of Medicine, Soonchunhyang University, 366-1 Ssangyong-dong, Cheonan, Chungnam 330-090, Republic of Korea

Received 11 February 2011; received in revised form 29 September 2011; accepted 1 October 2011
Available online 28 October 2011

Abstract

In this study, needle-shape TiO_2 fibers were successfully fabricated inside a micro-channeled Al_2O_3–ZrO_2 composite porous membrane system using sol–gel method. The micro-channeled Al_2O_3–ZrO_2 composite was fabricated using the fibrous monolithic (FM) process. Pure anatase phase TiO_2 was crystallized from the as-coated amorphous phase during calcination at 510 °C. The TiO_2 fibers grew on the surface frame of the micro-channeled Al_2O_3–ZrO_2 composite membrane and fully covered the inside of the micro-channeled pores. The specific surface area of the TiO_2 coated membrane system was dramatically increased by over 100 fold compared to that of the non-coated system. The photocatalytic activity of the membrane was also assessed and was shown to very effectively convert organic materials. Thus, this novel membrane holds promise for use as an advanced filtration system.

Keywords: A. Extrusion; A. Sol–gel processes; B. Fibers; D. TiO_2; E. Membranes

1. Introduction

TiO_2 has been shown to have excellent photocatalytic activity, high oxidation resistance abilities, long-term stability and low toxicity.[1] Many methods have been developed to decompose various pollutants such as water and air pollutions, using the intrinsic properties of TiO_2.[2] However, there are some limiting factors to the wide spread use of TiO_2 including its powder morphology, particle size and low surface area.[3] There are several methods to fabricate TiO_2 such as ion doping, ionized cluster beam (ICB), tape casting, CVD, sputtering, sol–gel process. However, these methods also have certain disadvantages like limited tube structure, flat disc type or hard to remove the polymer crystal templates used as a substrate.[4–9] Dionysiou and Choi et al. have synthesized nanostructured TiO_2 films and membranes on different substrates and for efficient use of photocatalysis.[10,11] They investigated the sol–gel process among others for the development of nanocystalline photocatalytic TiO_2 thin films and particles with modification.[12]

It is believed that the extent of the reaction at the solid gas interface depends on the total surface area. Thus, for a filtration system to be effective, its surface area should be high. Nano phase materials typically have a very high specific surface area due to their small size. This means that a small amount of material can produce a very high reactive surface area. Therefore, there is a high demand for coating materials with these fine particles. These materials typically need a carrier so that they can withstand dynamic loading and wear and tear. Thus, a novel method is needed to increase the active surface area of filtration systems as well as a robust substrate that will provide mechanical stability.

Previous studies have attempted to develop hollow membranes, which have high mechanical properties such as hardness, strength and toughness. The Al_2O_3/ZrO_2 ceramic composite system has been used in many applications including grinding and cutting tools, electric industries, high-performance filters, self-cleaning membrane systems as well as high-loaded biomaterials and catalysis substrates.[13–17] This composite has been widely used because it displays high mechanical properties, chemical resistance and wear resistance properties. Despite these advantages, this composite does have low fracture toughness, which is common for all ceramic based systems.[18–22] However, microstructural modifications

* Corresponding author. Tel.: +82 41 570 2427; fax: +82 41 570 2430.
E-mail address: lbt@sch.ac.kr (B.-T. Lee).

0955-2219/$ – see front matter © 2011 Elsevier Ltd. All rights reserved.
doi:10.1016/j.jeurceramsoc.2011.10.010

have allowed researchers to increase the fracture toughness of the Al_2O_3/ZrO_2 ceramic composite system and these designs have been incorporated into various geometric configurations including channelized porous systems. In our previous work, we developed an Al_2O_3/ZrO_2 ceramic composite system containing a channelized multilayered microstructure that could support high fluid flow and was stronger than the conventional porous system.[23] The surface on the inside of the channel was rough and could support further coating. Hence, a well-tailored multi-layered porous Al_2O_3/ZrO_2 composite system assisted by fibrous monolithic (FM) process could further improve the strength and fracture toughness dramatically.

In this study, the FM process was used to fabricate a multi-layered porous Al_2O_3/ZrO_2 composite, which was then used as a substrate for the fabrication of a hollow membrane system. Sol–gel coating and aging processes were used to obtain fine TiO_2 fibers, which improved the specific surface area. The detailed microstructural organization and photocatalytic activity of the membrane were evaluated.

2. Materials and methods

2.1. Fabrication of the micro-channeled Al_2O_3–ZrO_2 composite membrane substrates

The starting powders used in the experiment were Al_2O_3 (AKP-50, 300 nm, Sumitomo, Japan), monoclinic Zirconia (m-ZrO_2) (TZ-0Y, 80 nm, Tosoh, Japan) and tetragonal Zirconia (t-ZrO_2) (TZ-3Y, 80 nm, Tosoh, Japan). Carbon powder (<15 μm, Aldrich, USA) was used as a pore forming agent. Al_2O_3 powder with a 25 vol% of m-ZrO_2 was ball mixed for 24 h to create a homogeneous mixture. The ball-mixed Al_2O_3–(25% m-ZrO_2) powder, t-ZrO_2 powder and carbon powder were all shear-mixed separately with a polymer binder (Ethylene Vinyl Acetate (EVA) (Elvax 250 and Elvax 210, Dupont, USA)) in a heated blender (Shina Platec. Co., Suwon, South Korea) at a temperature of 120 °C. Stearic acid (Daejeon chemical company, Korea) was used to decrease the viscosity and enhance fine mixing. The polymer laden powders were then extruded in a heated die to obtain green filaments that were 1.5 mm in diameter and 8 mm in length. A total 5 alternate layers of t-ZrO_2 and Al_2O_3 (25% m-ZrO_2) filaments made the outer part of the arrangement. The arrangement was warm pressed and extruded at 120 °C at a speed of 7 mm/min. The 1st passed filaments were 3.5 mm in diameter. 61 1st passed filaments were reloaded in the same extrusion die and then extruded to obtain the 2nd passed filaments, which were 3.5 mm in diameter. The polymer binder was removed under a flow of nitrogen and then carbon was burnt out at 1000 °C in an air atmosphere. The samples were then sintered at 1500 °C for 2 h in air. The microstructure of the composites was examined using SEM (FE-SEM, JSM 6335F, JEOL, Tokyo, Japan).

2.2. Fabrication of micro-channeled Al_2O_3–ZrO_2/TiO_2 composite membrane

Commercial titanium tetra-isopropoxide (TTIP, Junsei Chemical Co., Ltd., Japan) was used as a precursor material for the TiO_2 sol–gel coating process. First, the molar ratio of mixed TTIP, 2-isopropanol (DEA, Samchun Pure Chemical Co., Ltd., Korea), diethanolamine (DEA, Samchun Pure Chemical Co., Ltd., Korea), and de-ionized water solution was 1:40:0.6:3.3, S. Kuai et al.[21] The multi-layered porous Al_2O_3/ZrO_2 composite membrane substrates were then immersed into the sol and stirred for 10 min. After immersion, micro-channeled Al_2O_3–ZrO_2/TiO_2 composite membrane substrates were covered with TiO_2 gel and removed from the TiO_2 solution. Later, the micro-channeled Al_2O_3–ZrO_2/TiO_2 composite membrane was washed with de-ionized water several times. The amorphous micro-channeled Al_2O_3–ZrO_2/TiO_2 composite membrane was calcined at 510 °C in the air to create the crystallized anatase TiO_2 phase. The crystallized micro-channeled Al_2O_3–ZrO_2/TiO_2 composite membrane was immersed in a warm 20% aqueous NaOH solution at 60 °C for 48 h in order to grow TiO_2 nano fibers. Finally, the micro-channeled Al_2O_3–ZrO_2/TiO_2 composite membrane was washed using de-ionized water several times and placed in an oven for drying at 60 °C.

The XRD (CuKα, D/MAX-250, Rigaku, Japan) technique was used to identify the crystalline phases of the membranes. The detail microstructure and morphology of the TiO_2 fibers in the fabricated micro-channeled Al_2O_3–ZrO_2/TiO_2 composite membrane substrates were investigated using FE-SEM (JSM-635F, JEOL, Japan). The decomposition efficiency was obtained from the decomposition of methyl orange (MO) and methylene blue (MB) at different UV irradiation times using a UV–visible spectrometer (DU® 800, Beckman Coulter, USA).

3. Results

3.1. SEM micrographs of micro-channeled Al_2O_3–ZrO_2 composite membrane

Fig. 1 shows SEM micrographs of the micro-channeled Al_2O_3–ZrO_2 composite membrane. The dark contrast regions in Fig. 1(b) are the Al_2O_3–(m-ZrO_2) layers and the bright contrast regions are the t-ZrO_2 layers. The pore size of the micro-channeled Al_2O_3–ZrO_2 composite membrane ranged between 150 and 200 μm and the total diameter of the micro-channeled Al_2O_3–ZrO_2 composite membrane was 2.5 mm. In this study, the thickness was less than 2 mm while the diameter was 2.5 mm. But these parameters such as pore size, pore distribution and thickness are easy to control using our FM process because the Al_2O_3–ZrO_2 composite section used in this study was cut from a long body. The thickness was arbitrarily set according to the experiments.

The polymer and carbon, which were used as the binder and pore forming agent, respectively, were completely removed during the burn-out process and a dense composites system was obtained after sintering. The small filament diameter was chosen to facilitate the extrusion process. Other diameters can also be used depending on the desired design. A rough pore surface resulted from the removal of the carbon/polymer composite, which was used as a pore-forming agent (Fig. 1(b)). On the other hand, the frame region had a smooth surface and

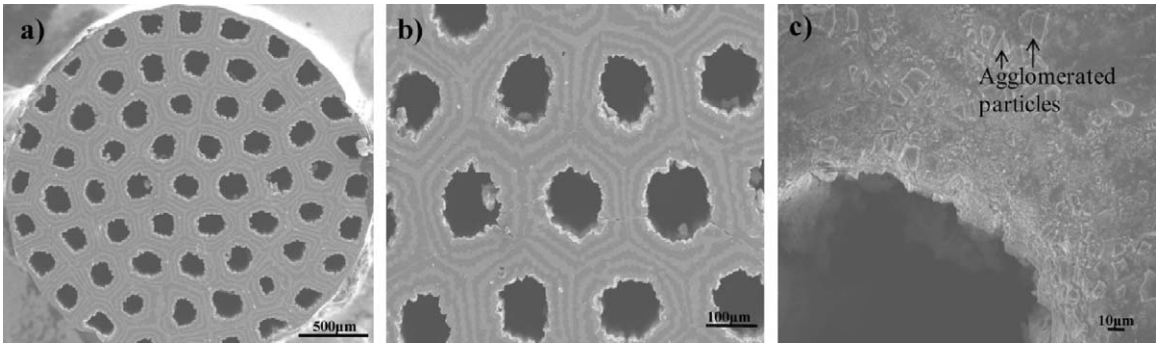

Fig. 1. SEM micrographs of (a) micro-channeled Al_2O_3–ZrO_2 composite membrane used as a substrate, (b) high magnification of (a), and (c) TiO_2 fibers after coating.

bulk defects such as shrinkage or large/micro cracks were not observed on the micro-channeled Al_2O_3–ZrO_2 composite membrane after sintering as shown in Fig. 1(a) and (b). The entire channeled Al_2O_3–ZrO_2 composite membrane was covered with amorphous TiO_2 when the sol–gel method was used. Some agglomerated TiO_2 particles were observed on the surface of the composite membrane, which occurred during drying after sol–gel coating at room temperature (Fig. 1(c)).

3.2. SEM micrographs of TiO_2 fibers on the micro-channeled Al_2O_3–ZrO_2/TiO_2 composite membrane

Fig. 2 shows SEM micrographs of the TiO_2 fibers on the micro-channeled Al_2O_3–ZrO_2/TiO_2 composite membrane after calcinations at 510 °C and aging for 48 h. In Fig. 2(a), the P region is the pore part and the Q region is the frame part of the micro-channeled Al_2O_3–ZrO_2/TiO_2 composite membrane, which is shown in more detail in Fig. 2(b) and (c). The frame and pore part of the micro-channeled Al_2O_3–ZrO_2 composite membrane was completely soaked in the TiO_2 sol and was strongly attached to the membrane. Needle-shape thin fibers and thick fibers were mixed with each other and covered the entire pore surface of the micro-channeled Al_2O_3–ZrO_2/TiO_2 composite membrane as shown in the P region in Fig. 2(b). The frame part was also fully covered with TiO_2 fibers after the aging process as shown in the Q region of Fig. 2(c). The TiO_2 fibers were randomly spread on the micro-channeled Al_2O_3–ZrO_2/TiO_2 composite membrane. The morphology and direction of the fibers can be more clearly seen in the high magnification image of Fig. 2(d). The EDS spectrum in Fig. 2(d) shows the elemental profiles of the surface after coating. Al and Zr elements, which were used in the Al_2O_3–ZrO_2 substrates, and Ti element, which were used for the TiO_2 coating, were detected (Fig. 2(d)).

3.3. XRD profiles of as synthesized and calcined TiO_2 powder

Fig. 3 shows the XRD profiles of the as synthesized TiO_2 powder (a) and calcined at 510 °C and aged for 48 h (b). When TiO_2 powders were calcined at 510 °C for 2 h at heating rate of 5 °C/min, crystalline phases were detected and all crystalline phases were found to be in the anatase TiO_2 phase. No adverse phase transformations were detected and only the pure anatase phase was detected in the XRD during the calcination process as shown in Fig. 3(b). The TiO_2 powder and fibers used for XRD observation were collected by crushing the micro-channeled Al_2O_3–ZrO_2/TiO_2 composite membrane into a fine powder using a mortar.

3.4. Surface area of TiO_2 coated and non-coated Al_2O_3–ZrO_2 composite membrane

Fig. 4 shows the TiO_2 coated and non-coated Al_2O_3–ZrO_2 composite membrane fabricated using the mercury intrusion porosimetry (MIP) method. TiO_2 non coated Al_2O_3–ZrO_2 composite membrane had a very low specific surface area (0.000138 m^2/g). In comparison, the TiO_2 coated Al_2O_3–ZrO_2 composite membrane that was subjected to the calcination and aging process showed a significantly higher specific surface area (0.0152 m^2/g). The TiO_2 coated Al_2O_3–ZrO_2 composite membrane (Fig. 4(b)) had a large surface area due to the incorporation of TiO_2 particles attached to the wall of Al_2O_3–ZrO_2 composites. Fig. 5 shows the pore size distribution in terms of mercury intrusion through the pores for both non coated and coated sample. As predicted the coated sample contained a continual mercury intrusion that was 4 μm in dimension. The intrusion volume at a lower diameter represents mainly the inter-particle spacing t of the deposited and grown TiO_2 fibers.

3.5. Photocatalytic activity and performance evaluation

Fig. 6 shows the photocatalytic activities of the micro-channeled Al_2O_3–ZrO_2/TiO_2 composite membrane after calcination at 510 °C and aging for 48 h in a 20% NaOH solution, which contained fully developed anatase phase TiO_2 fibers. The decomposition of methyl orange (MO) and methylene blue (MB) in the calcined membrane at 510 °C was time dependent and the concentration of the organic materials was quickly reduced within a few minutes. After 4 h, almost 95% of MO and 90% of the MB solution were decomposed. The reference solution (not containing the micro-channeled Al_2O_3–ZrO_2/TiO_2 composite membrane) did not change at all during the entire irradiation treatment. The residual concentration of MO in the

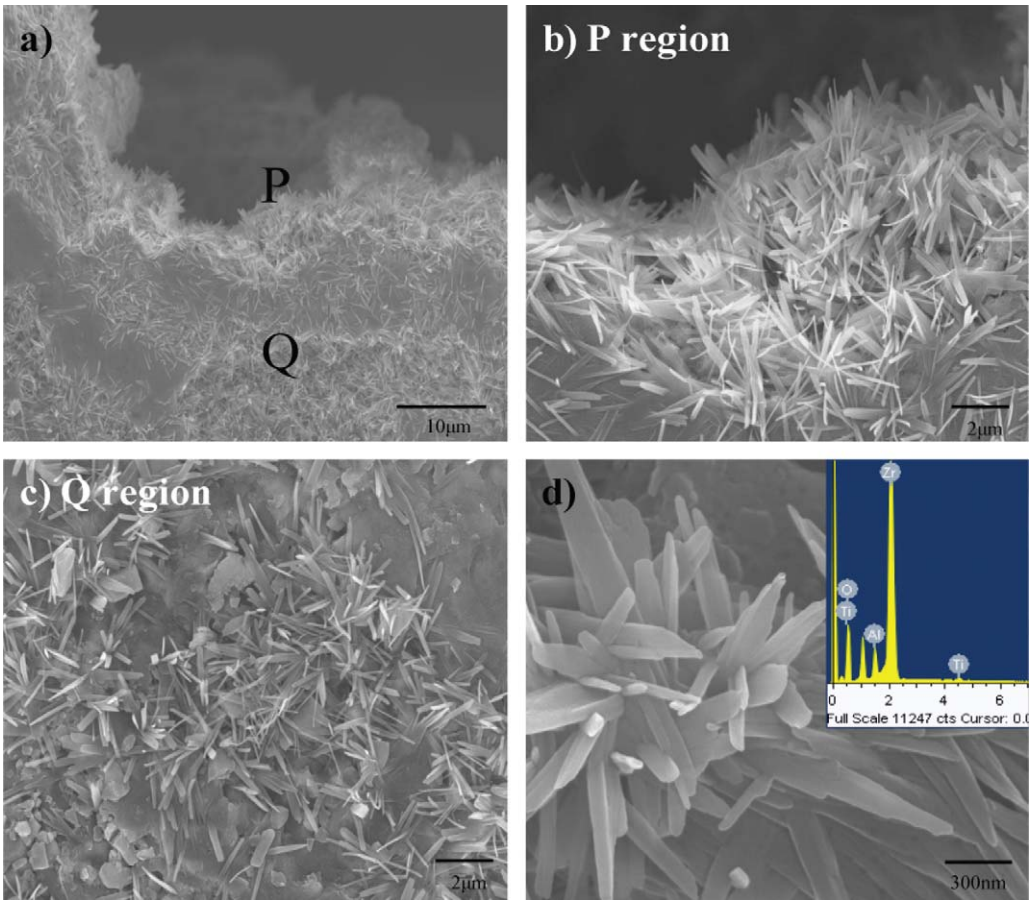

Fig. 2. SEM micrographs of (a) inside the pore (P region), (b) high magnification of (a), (c) frame part (Q region) and (d) high magnification of TiO_2 fibers and their EDS profile.

calcined composite membrane was dramatically decreased to almost 0% after 8 h of UV irradiation. Thus, this composite membrane showed a high decomposition efficiency under UV irradiation. These results indicate that the calcined micro-channeled Al_2O_3–ZrO_2/TiO_2 composite membrane could easily and effectively decompose organic materials.

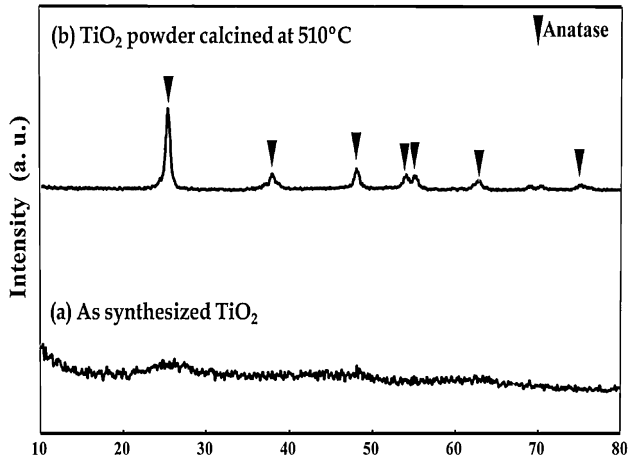

Fig. 3. XRD profiles of (a) the as synthesized TiO_2 powder and powders calcined at (b) 510 °C.

4. Discussions

In this study, a micro-channeled Al_2O_3–ZrO_2 composite system was used as a substrate material to produce a mechanically robust composite membrane system with catalytically active materials. The Al_2O_3/ZrO_2 multilayer system containing micro-channels was sintered at 1500 °C and had a densified structure. The pore surface of the membrane was very rough and these rough pore surfaces can be easily coated with various other materials. The layered structure of the alternated Al_2O_3–(m-ZrO_2) and t-ZrO_2 laminates produces alternate compressive and tensile residual stresses along the layers. The compressive stress in the micro-channeled Al_2O_3–(m-ZrO_2) layers has a strengthening effect and can improve the fracture toughness of the composites. The alternate compressive layer and tensile layer are responsible for crack arresting and crack deflection because of its unidirectionally aligned concentric laminated microstructure.[23] The rough surface inside the pore channel is due to the repeated extrusion of the green composites (the core/shell structure was repeated four times during the extrusion process).

As shown in Fig. 2(b) and (d), the surface morphology was dramatically changed before and after TiO_2 coating compared with Fig. 1(a) and (b). The TiO_2 fibers grew on the Al_2O_3–ZrO_2 scaffold TiO_2 coated layer as shown in Fig. 2(a)

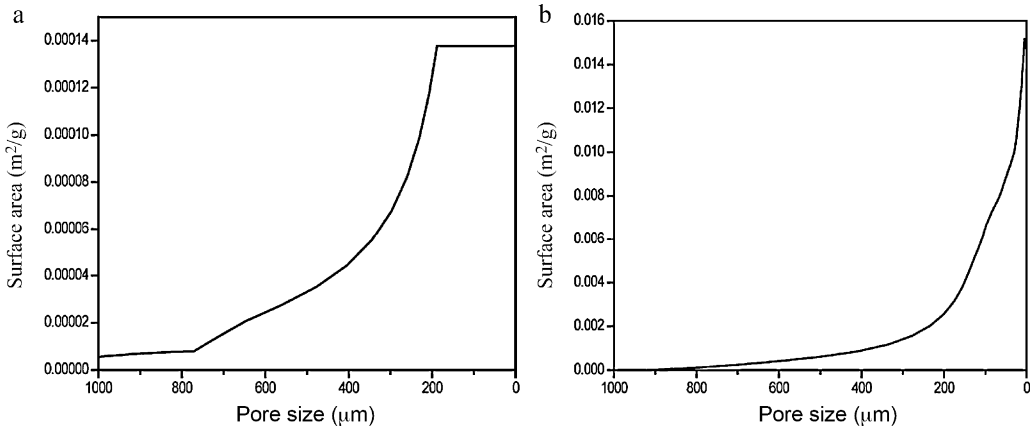

Fig. 4. Surface area vs. pore size of (a) TiO_2 non coated and (b) TiO_2 coated Al_2O_3–ZrO_2 composite membrane.

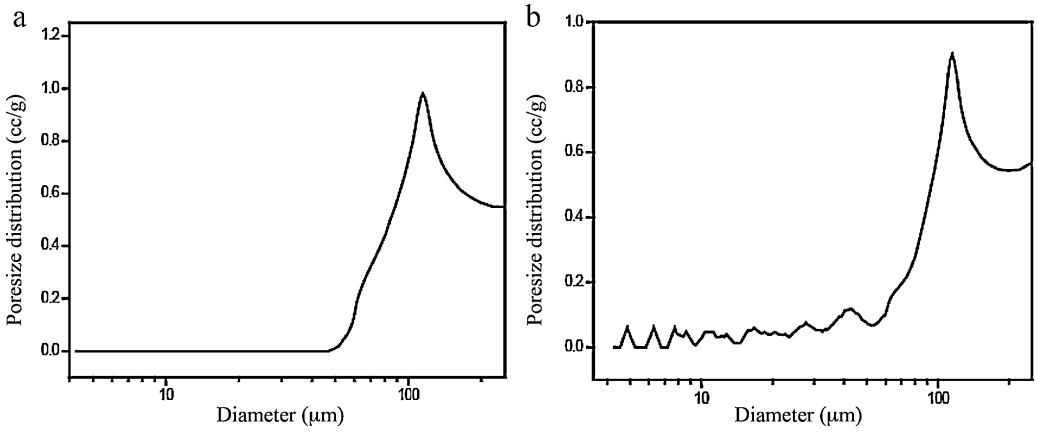

Fig. 5. Pore size distribution in terms of mercury intrusion for (a) TiO_2 non coated and (b) TiO_2 coated Al_2O_3–ZrO_2 composite membrane.

when the micro-channeled Al_2O_3–ZrO_2/TiO_2 composite membrane was treated with NaOH aqueous solution and washed with de-ionized water. It has been shown that when micro-channeled Al_2O_3–ZrO_2/TiO_2 composite membranes are treated with NaOH aqueous solution some of the Ti–O–Ti bonds are broken and new Ti–O–Na and Ti–OH bonds begins to form. The Ti–O–Na and Ti–OH bonds have been reported to react with water to form new Ti–O–Ti bonds. At this stage, the metastable anatase phase begins form at temperatures as low as 60 °C.[24–27]

As shown in Fig. 3(a), no crystalline phases were detected in the as synthesized TiO_2 (as-coated condition) powder since it was in an amorphous phase (non-calcined state). The purity of the anatase phase is crucial for photocatalytic activity. The rutile phase does not strongly influence the photocatalytic activity, while the anatase phase has a great effect on photocatalytic activity. In this study, only the anatase phase was detected (Fig. 3(b)).

In the case of commercial TiO_2 coated membranes, which have a smooth surface, pollutants are passed through in just a one-way direction (right to left or left to right, red arrow) as shown in Fig. 7(a). On the other hand, if membranes have a rough surface due to needle-shaped TiO_2 fibers, which was the case for the micro-channeled Al_2O_3–ZrO_2/TiO_2 composite membrane (as shown in Fig. 2), pollutant materials can easily come in contact with TiO_2 on the membrane and be passed in all directions (including right, left, up and down direction) as shown in Fig. 7(b). This phenomenon would lead to an increase in the number of contacts between the pollutant materials and active sites on the substrate and increase the efficiency of the membrane. The TiO_2 fibers, which were grown on the micro-channeled Al_2O_3–ZrO_2/TiO_2 composite membrane, produced

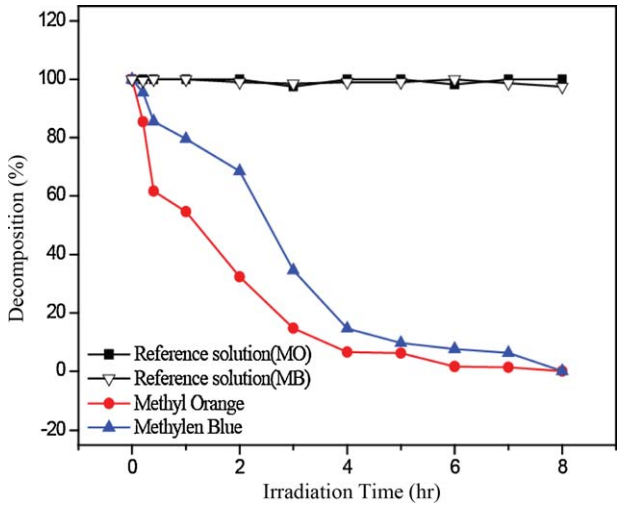

Fig. 6. Photocatalytic activities of the micro-channeled Al_2O_3–ZrO_2 composite membrane.

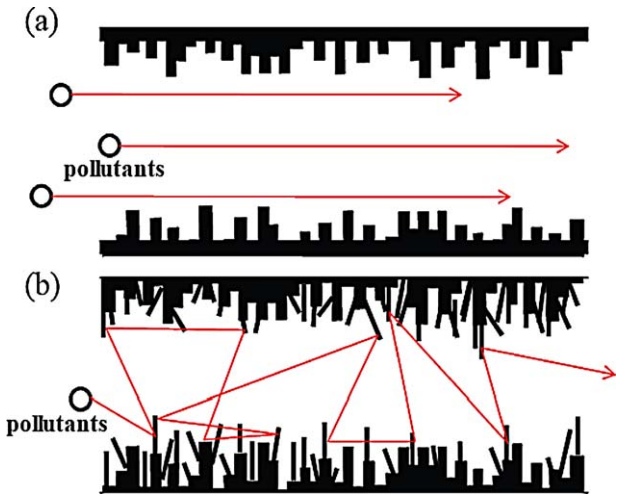

Fig. 7. (a) Schematic diagram of (a) normal porous body and (b) rough porous body using the FM process.

a very rough surface and dramatically increased the surface area. When pollutant materials were passed through the micro-channeled Al_2O_3–ZrO_2/TiO_2 composite membrane, it had many chances to come in contact with catalysts material (TiO_2) and could decompose faster compared with common porous membranes.

The pore diameter vs. specific surface area shown in Fig. 4 demonstrates that coating with TiO_2 abruptly changed the surface area of the membrane. TiO_2 coated Al_2O_3–ZrO_2 composite membrane (Fig. 4(b)) had a large surface area due to the broad pore size distribution. These values indicate that the TiO_2 coated Al_2O_3–ZrO_2 composite membrane had a rough surface due to the formation of TiO_2 fibers during the aging process in the reaction solution (20% NaOH solution). From Fig. 4(b), it was evident that the surface roughness as well as the surface area improved due to an increase in the inter fiber gap. This can be seen by the quick increase from around 200 to 100 μm in pore diameter. Another increase was observed when the pore diameter changed in the 40–10 μm range. These values demonstrate that that TiO_2 fiber dramatically increased the specific surface area by around 100 fold compared to the non-coated example.

The effect of the nano fibers on the surface area was demonstrated by the differential mercury intrusion with respect to the pore diameter as shown in Fig. 5 While the non-coated sample showed no mercury intrusion due to the non-availability of porous space, the coated sample, showed mercury intrusion down to 4 m. This too indicates that the inter-particle porosity was widely distributed due to the coating process.

In the photocatalytic assay, the TiO_2 anatase phase was shown to affect the degradation of organic materials such as the methyl orange (MO) and methylene blue (MB) solution, which were used as a reference solution (Fig. 5(b)). And when we evaluated the photocatalytic activity, the MO solution was circulated, which indicated that there were no issues the permeation properties. Moreover, the channel of the Al_2O_3–ZrO_2 composite body traversed the entire composite, which ensured passage of the working liquid.

Photocatalytic materials such as TiO_2 are considered an n-type semiconductor. Under UV irradiation, an electron and hole were formed from the conduction-band and valence-band, respectively. Conduction-band electrons and valence-band holes migrated on the surface and recombined with oxygen and hydroxyl, respectively. These recombination produced super oxide anions and hydroxyl radicals (OH radicals), which was the driving force behind the decomposition of the organic materials.[7,28]

5. Conclusion

Using the micro-channeled Al_2O_3–ZrO_2 composite, a TiO_2 coated micro-channeled Al_2O_3–ZrO_2 composite membrane was fabricated using a combination of sol–gel and aging processes. The microstructure, membrane morphology and photocatalytic decomposition efficiency was investigated. The micro-channeled Al_2O_3–ZrO_2 composite was used as a substrate for the fabrication of a membrane by the FM process and this composite was shown to dramatically increase the strength and fracture toughness of porous bodies. TiO_2 particles homogeneously coated the pore and frame part of the micro-channeled Al_2O_3–ZrO_2 composite and was calcined at 510 °C. The aging process was carried out for 48 h in a 20% NaOH solution at 60 °C in the oven to convert the particles into fibers. The fabricated photocatalytically active membrane showed high performance in degrading organic solvents; thus, it holds great promise for use as a high performance functional membrane.

References

1. Yun J, Jin D, Lee Y-S, Kim H-I. Photocatalytic treatment of acidic waste water by electrospun composite nanofibers of pH-sensitive hydrogel and TiO_2. *Materials Letters* 2010;**64**:2431–4.
2. Hoffmann MR, Martin ST, Choi W, Bahnemann DW. Environmental applications of semiconductor photocatalysis. *Chemical Reviews* 1995;**95**:69–96.
3. Khanna PK, Singh N, Charan S. Synthesis of nano-particles of anatase-TiO_2 and preparation of its optically transparent film in PVA. *Materials Letters* 2007;**61**:4725–30.
4. Fukushima K, Yamada I. Surface smoothness and crystalline structure of ICB deposited TiO_2 films. *Applied Surface Science* 1989;**43**:32–6.
5. György E, Socol G, Axente E, Mihailescu IN, Ducu C, Ciuca S. Anatase phase TiO_2 thin films obtained by pulsed laser deposition for gas sensing applications. *Applied Surface Science* 2005;**247**:429–33.
6. Jingxian Z, Dongliang J, Weisensel L, Greil P. Binary solvent mixture for tape casting of TiO_2 sheets. *Journal of the European Ceramic Society* 2004;**24**:147–55.
7. Xie H, Zhu L, Wang L, Chen S, Yang D, Yang L, et al. Photodegradation of benzene by TiO_2 nanoparticles prepared by flame CVD process. *Particuology* 2011;**9**:75–9.
8. Sung Y-M, Kim H-J. Sputter deposition and surface treatment of TiO_2 films for dye-sensitized solar cells using reactive RF plasma. *Thin Solid Films* 2007;**515**:4996–9.
9. Mohammadi MR, Fray DJ. Nanostructured TiO_2–CeO_2 mixed oxides by an aqueous sol–gel process: effect of Ce:Ti molar ratio on physical and sensing properties. *Sensors and Actuators B: Chemical* 2010;**150**:631–40.
10. Yoo KS, Choi H, Dionysiou DD. Synthesis of anatase nanostructured TiO_2 particles at low temperature using ionic liquid for photocatalysis. *Catalysis Communications* 2005;**6**:259–62.

11. Choi H, Stathatos E, Dionysiou DD. Photocatalytic TiO_2 films and membranes for the development of efficient wastewater treatment and reuse systems. *Desalination* 2007;**202**:199–206.
12. Choi H, Stathatos E, Dionysiou DD. Synthesis of nanocrystalline photocatalytic TiO_2 thin films and particles using sol–gel method modified with nonionic surfactants. *Thin Solid Films* 2006;**10**:107–14.
13. Sarkar SK, Lee BT. Evaluation and comparison of the microstructure and mechanical properties of fibrous Al_2O_3–(m-ZrO_2)/t-ZrO_2 composites after multiple extrusion steps. *Ceramics International* 2010;**36**:1971–6.
14. Zhao X, An Y, Chen J, Zhou H, Yin B. Properties of Al_2O_3–40 wt.% ZrO_2 composite coatings from ultra-fine feedstocks by atmospheric plasma spraying. *Wear* 2008;**265**:1642–8.
15. Chang Q, Zhang L, Liu X, Peng D, Meng G. Preparation of crack-free ZrO_2 membrane on Al_2O_3 support with ZrO_2–Al_2O_3 composite intermediate layers. *Journal of Membrane Science* 2005;**250**:105–11.
16. Ewais EMM, Attia MAA, Abousree-Hegazy A, Bordia RK. Investigation of the effect of ZrO_2 and ZrO_2/Al_2O_3 additions on the hot-pressing and properties of equimolecular mixtures of α- and β-Si_3N_4. *Ceramics International* 2010;**36**:1327–38.
17. Daguano JKMF, Santos C, Souza RC, Balestra RM, Strecker K, Elias CN. Properties of ZrO_2–Al_2O_3 composite as a function of isothermal holding time. *International Journal of Refractory Metals and Hard Materials* 2007;**25**:374–9.
18. Jin P, Miao L, Tanemura S, Xu G, Tazawa M, Yoshimura K. Formation and characterization of TiO_2 thin films with application to a multifunctional heat mirror. *Applied Surface Science* 2003;**212–213**:775–81.
19. Lee B-T, Lee K-H, Hiraga K. Stress-induced phase transformation of ZrO_2 in ZrO_2 (3 mol%Y_2O_3)–25 vol%Al_2O_3 composite studied by transmission electron microscopy. *Scripta Materialia* 1998;**38**:1101–7.
20. Lim JI, Yu B, Woo KM, Lee Y-K. Immobilization of TiO_2 nanofibers on titanium plates for implant applications. *Applied Surface Science* 2008;**255**:2456–60.
21. Kuai SL, Hu XF, Truon VV. Synthesis of thin film titania photonic crystals through a dip-infiltrating sol–gel process. *Journal of crystal growth* 2003;**259**:404–10.
22. Xu Q-C, Wellia DV, Sk MA, Lim KH, Loo JSC, Liao DW, et al. Transparent visible light activated C–N–F-codoped TiO_2 films for self-cleaning applications. *Journal of Photochemistry and Photobiology A: Chemistry* 2010;**210**:181–7.
23. Lee BT, Sarkar SK. Fabrication of super-high-strength microchanneled Al_2O_3–ZrO_2 ceramic composites with fibrous microstructure. *Scripta Materialia* 2009;**61**:686–9.
24. Kuai S, Badilescu S, Bader G, Brüning R, Hu X, Truong VV. Preparation of large-area 3D ordered macroporous titania films by silica colloidal crystal templating. *Advanced Materials* 2003;**15**:73–5.
25. Chen Q, Zhou W, Du GH, Peng LM. Trititanate nanotubes made via a single alkali treatment. *Advanced Materials* 2002;**14**:1208–11.
26. Kasuga T, Hiramatsu M, Hoson A, Sekino T, Niihara K. Titania nanotubes prepared by chemical processing. *Advanced Materials* 1999;**11**:1307–11.
27. Chu C-L, Hu T, Zhou J, Pu Y-P, Yin L-H, Dong Y-S, et al. Effects of H_2O_2 pretreatment on surface characteristics and bioactivity of NaOH-treated NiTi shape memory alloy. *Transactions of Nonferrous Metals Society of China* 2006;**16**:1295–300.
28. Chen J, Zhang J, Xian Y, Ying X, Liu M, Jin L. Preparation and application of TiO_2 photocatalytic sensor for chemical oxygen demand determination in water research. *Water Research* 2005;**39**:1340–6.